

Magnetic equilibria during enhanced plasma performance phases in Wendelstein 7-X stellarator

E. V. Hausten¹, K. Rahbarnia¹, H. Thomsen¹, C. Brandt¹, U. Neuner¹, C. Büschel¹, S. V. Mendes¹, S. A. Lazerson² and the Wendelstein 7-X Team [1]

¹ Max Planck Institute for Plasma Physics Greifswald, Germany

² Gauss Fusion GmbH, Germany

In experiments at the Wendelstein 7-X (W7-X) stellarator, additional plasma fueling with frozen hydrogen pellets has been shown to lead to a phase of significantly improved plasma parameters. This phase lasts only for a few confinement times and is characterized by enhanced plasma pressure p , ion temperature T_i and global energy confinement time τ_{conf} [2]. The enhanced performance (high plasma $\beta = \frac{2\mu_0 p}{B^2}$ with vacuum permeability μ_0 and magnetic field strength B) might be related to strong density gradients which stabilize ion temperature gradient modes [2]. In some experimental programs, sudden crashes of the diamagnetic energy W_{dia} are observed within the high β phase. These events are potentially caused by changes in the rotational transform ι and might accelerate the confinement degradation. In this contribution we investigate the magnetohydrodynamic (MHD) equilibria for a pellet-fueled experiment before and during the high β phase and with respect to crashes of W_{dia} . We compare the results to alternative enhanced β scenarios, which combine electron cyclotron resonance heating (ECRH) and neutral beam injection (NBI).

Equilibrium reconstruction with STELLOPT

In order to determine the equilibrium as accurately as possible, we perform reconstructions with the STELLOPT code [4]. We take into account multiple experimental measurements, including magnetic signals of fluxloops and Rogowski coils [5], density n and temperatures $T_{e,i}$ of electrons and ions provided by Thomson scattering [6] and XICS diagnostics [7]. A recent extension of STELLOPT incorporates soft X-ray emissivity measurements provided by the XMCTS diagnostic [8], improving the fidelity of the reconstruction. STELLOPT iteratively solves the MHD force balance equation using VMEC [9], forward-models diagnostic signals and compares them to experimental measurements. The aim is to adjust the force balance and boundary conditions such that the discrepancy of modeled and measured signals is minimized and the obtained equilibrium is in good agreement with the experiment.

Experiment overview

During recent experimental campaigns at W7-X high plasma β has been achieved in different

magnetic configurations and employing different heating strategies. We have selected three scenarios for detailed reconstructions (shown in Fig. 1):

- A) High ι FTM configuration ($\iota_{LCFS} = \frac{6}{5}$) at $\langle B_0 \rangle = -2.3$ T with a pellet injection phase and combined NBI and ECRH O2 mode heating.
- B) Intermediate ι FMM configuration at $\langle B_0 \rangle = 2.4$ T, starting with ECRH X2 mode heating followed by a pure NBI phase and ECRH re-introduction in O2 mode.
- C) Standard configuration EIM ($\iota_{LCFS} = \frac{5}{5}$) at $\langle B_0 \rangle = -1.7$ T (lowered B-field) with NBI heating followed by ECRH X3 mode take over [10].

ι_{LCFS} describes ι at the last close flux surface and $\langle B_0 \rangle$ the average magnetic field on axis.

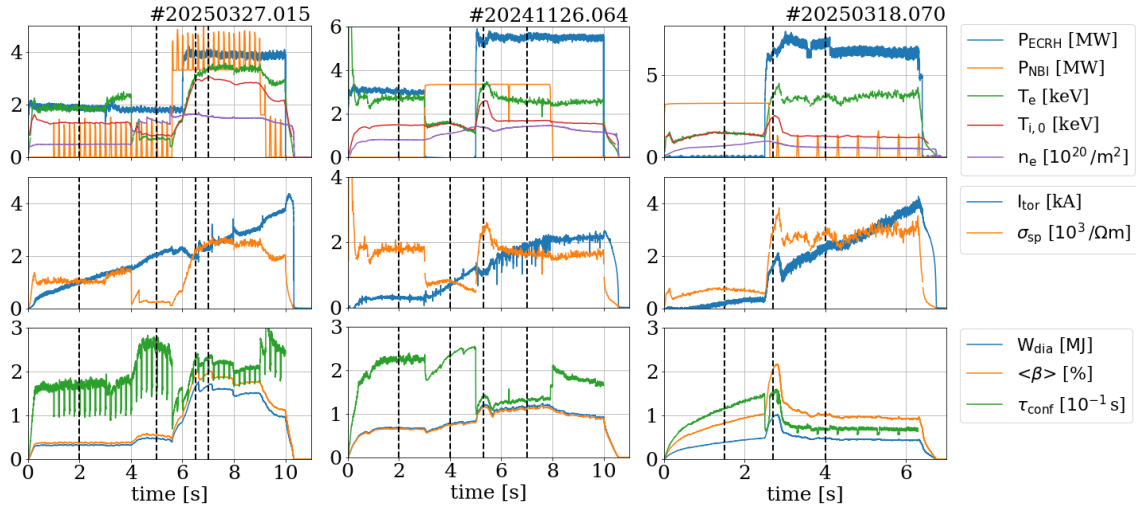


Fig. 1: Timeline of high β scenarios A (left), B (centre) and C (right) with corresponding heating power P , temperatures, density, diamagnetic energy, confinement time and toroidal current I_{tor} . Also shown are the approximated Spitzer conductivity $\sigma_{sp} \approx 400 T_e^{1.5}$ and volume averaged β derived as $\langle \beta \rangle \approx \frac{3\mu_0 W_{dia}}{4V_0 \langle B_0 \rangle^2}$. The vertical dashed lines mark the time points chosen for equilibrium reconstructions.

Shafranov shift

An important finite β effect on the equilibrium is the outward shift of magnetic flux surfaces, called Shafranov shift. Pressure gradients within the plasma give rise to Pfirsch-Schlüter currents. These create an additional vertical magnetic field, which causes the flux surfaces to shift. The strength of the Shafranov shift can be characterized by the shift of the magnetic axis. In low β and low shear limit the axis shift is expected to depend linearly on β_0 (plasma β on axis) and on $1/\iota^2$ (i.e. on the magnetic configuration) [11]. With the reconstructions we reproduce the axis shift strength with β_0 , as well as the tendency of smaller shifts in high ι configuration A, compared to small and intermediate ι configurations B and C (see Fig. 2, left). For illustration purposes the flux surface shift in experiment A is depicted in Fig. 2, right.

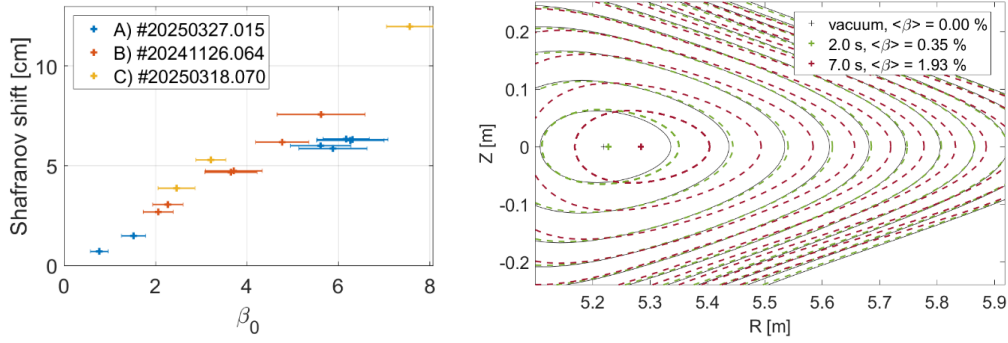


Fig. 2: Left: Reconstructed Shafranov shifts at different values of β_0 for experiments A-C. Right: Flux surface geometry (triangular-shaped plane) in the low- and high β phase of experiment A at time $t = 2.0$ s (green) and $t = 7.0$ s (red). The black lines correspond to vacuum geometry.

Rotational transform ι

Within an experiment, the radial profile of ι and its volume average vary mainly due to changes in the toroidal current I_{tor} and toroidal current density j . The main contribution to I_{tor} is associated to the bootstrap current which is largest in regions of strong pressure gradients. j is also dependent on the plasma conductivity and thereby on electron temperature, related to plasma pressure and β . For experiment A we verify the ι -profile change with I_{tor} and j displayed over the normalized flux s in Fig. 3, left and centre. Overall, I_{tor} tends to build up over time within the experiment, resulting in a systematic shift of also the volume averaged ι . This is also true for the experiments B and C (not shown in Fig. 3). In contrast, there seems to be no strong correlation between the volume averaged ι and plasma β (see Fig. 3, right). Note, that even minor changes in the ι -profile might cause the formation, vanishing or shifting of magnetic islands, thus affecting transport and stability characteristics of the plasma.

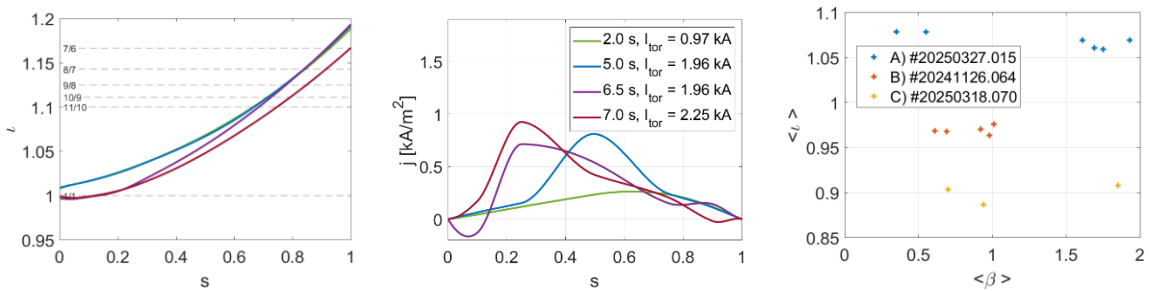


Fig. 3: ι -profile (left) and toroidal current density profile (centre) over normalized flux in experiment A at various points in time, corresponding to different values of total toroidal current. Also shown is the average ι for experiments A-C at different values of average β (right).

Crashes of diamagnetic energy W_{dia}

In experiment A, a series of sudden drops of W_{dia} are observed. The first and most prominent of these crashes occurs at ~ 6.6 s where W_{dia} drops by ~ 200 kJ on the time scale of ~ 1 ms. The event is also clearly visible in the Mirnov coil diagnostic, which measures magnetic field

fluctuations (see Fig. 4, left), as well as in the XMCTS diagnostic [12]. In reconstructed equilibria before and after the event we observe a sudden drop of the edge ι profile (Fig. 4, centre) due to an increase of I_{tor} and higher current density close to the edge. We find a flattening of the pressure profile (Fig. 4, right), caused by a flattening of the density.

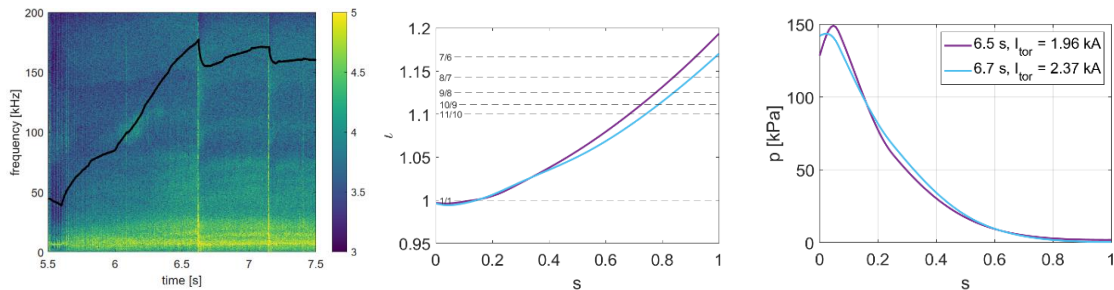


Fig. 4: Left: Frequency spectrum measured by Mirnov coil QXM11CE190 during experiment A. The black graph displays $W_{dia}/10$ [kJ].

Conclusion and outlook

We have investigated different high β scenarios recently achieved in W7-X by analyzing plasma equilibria at different phases of the experimental programs. The equilibria have been reconstructed using STELLOPT, taking into account soft X-ray measurements and a variable toroidal current profile. An analysis of the Shafranov shift and rotational transform is provided, demonstrating finite β effects and comparing between magnetic configurations. Furthermore, we have investigated equilibrium changes related to a crash in W_{dia} in a pellet-fueled experiment. Future work needs to focus on building up a larger set of reconstructed equilibria to reliably characterize finite β effects and non-linear trends among a broader configuration space. To obtain a more detailed picture of the flux surface geometry, the position and size of magnetic islands should be taken into account within the analysis.

References

- | | |
|---|---|
| [1] O. Grulke et al 2024 Nucl. Fusion 62 112002 | [7] N. A. Pablant 2021 Rev. Sci. Instrum 92 043530 |
| [2] S. A. Bozhenkov et al 2020 Nucl. Fusion 60 066011 | [8] C. Brandt et al 2020 Plasma Phys. Control. Fusion 62 035010 |
| [3] A. v. Stechow et al 2020 arXiv:2010.02160 | [9] S. P. Hirshman and J. C. Whitson 1983 Phys. Fluids 26 3553 |
| [4] S. A. Lazerson 2015 Nucl. Fusion 55 | [10] N. S. Polei et al, in preparation |
| [5] K. Rahbarnia et al 2018 Nucl. Fusion 58 096010 | [11] A. Weller et al 2009 Nucl. Fusion 49 065016 |
| [6] S. A. Bozhenkov et al 2017 JINST 12 P10004 | [12] H. Thomsen et al 2025 EPS conference |

This work has been carried out within the framework of the EUROfusion Consortium, funded by the European Union via the Euratom Research and Training Programme (Grant Agreement No 101052200 — EUROfusion). Views and opinions expressed are however those of the author(s) only and do not necessarily reflect those of the European Union or the European Commission. Neither the European Union nor the European Commission can be held responsible for them.